Supplemental Table of Contents:

Supplemental Table 1. The primers used for quantitative real time PCR and ChIP-PCR.

Supplemental figure 1. The expression of ferroptosis related genes was dysregulated in Pkd1 mutant renal epithelial cells and human ADPKD kidneys.

Supplemental figure 2. The expression of ferroptosis related genes was dysregulated in Pkd2 mutant kidneys.

Supplemental figure 3. Depletion of Pkd1 increases the sensitivity of cystic renal epithelial cells to erastin.

Supplemental figure 4. Treatment with erastin decrease GSH levels but increased cyst-lining epithelial cell proliferation in Pkd1RC/RC kidneys.

Supplemental figure 5. Treatment with erastin did not promote cyst growth in Pkd1RC/+ mice kidneys.

Supplemental figure 6. Mitochondrial morphological and function alteration in Pkd1 mutant kidneys treated with erastin or Fer-1.

Supplemental figure 7. Renal and systemic iron metabolism mediated by iron regulatory proteins (IRPs) and heme oxygenase-1 (HO-1) in Pkd1 mutant kidneys

Supplemental figure 8. Iron metabolism associated genes were dysregulated in Pkd1 mutation renal epithelial cells and tissues treated with erastin or Fer-1.

Supplemental figure 9. Pkd1 mutant renal epithelial cell proliferation was regulated by 4-HNE produced during ferroptotic process.

Supplemental figure 10. Pkd1 mutant renal epithelial cell proliferation was regulated by 4-HNE produced during ferroptotic process.

Supplemental figure 11. The expression of GPX4 was regulated by ATF3 in Pkd1 mutant renal epithelial cells.

Supplemental Table 1. The primers used for quantitative real time PCR and ChIP-PCR.

Genes	Forward primers (5'-3')	Reverse primers (5'-3')
Actin (mouse)	AAGAGCTATGAGCTGCCTGA	TACGGATGTCAACGTCACAC
GPX4 (mouse)	GCAATGAGGCAAAACTGACG	CTTGATTACTTCCTGGCTCCTG
SLC3A2 (mouse)	ACCTCACTCCCAACTACCAG	ATCAGCTTTCCCACATCCC
SLC7A11 (mouse)	TCTTCGATACAAACGCCCAG	TGATAAGAAAACCGACCCCG
Fpn (mouse)	TCTCTGTGATTGTGACCGTG	AATTTCCTTGCCCGTAGAGTC
TFR1 (mouse)	AGTGTCAGAAAACCCAAGAGG	CGTTTCAGCCAGTTTCACAC
HO-1 (mouse)	ACAGAGGAACACAAAGACCAG	GTGTCTGGGATGAGCTAGTG
DMT1 (mouse)	GGGTTGGCAGTGTTTGATTG	CTGGGCTGTTAGTCATCTGG
FTH1 (mouse)	CTTTGCAACTTCGTCGTTCC	AGGTTGATCTGGCGGTTG
ATF3 (mouse)	ATAAACACCTCTGCCATCGG	GCCTCCTTTTCCTCTCATCTTC
Actin (human)	ACCTTCTACAATGAGCTGCG	CCTGGATAGCAACGTACATGG
GPX4 (human)	GGGCTACAACGTCAAATTCG	TCGATGAGGAACTTGGTGAAG
SLC3A2 (human)	GGCAAAATATCACCAAGGGC	CCAGTAGAACCAGAATCAGACAG
SLC7A11 (human)	TTTTGTACGAGTCTGGGTGG	CGCAAGTTCAGGGATTTCAC
Fpn (human)	GGGTGGACAAGAATGCTAGAC	ATGGTACATGGTCAGAAGCTC
TFR1 (human)	ACTTGCCCAGATGTTCTCAG	GTATCCCTCTAGCCATTCAGTG
HO-1 (human)	TCAGGCAGAGGGTGATAGAAG	TTGGTGTCATGGGTCAGC
DMT1 (human)	TGGAGATCATGGGGAGTCTG	AAGAAAACCTGGTCCGGTGAA
FTH1 (human)	CTCCTACGTTTACCTGTCCATG	TTTCTCAGCATGTTCCCTCTC
ATF3 (human)	AGAAGGAACATTGCAGAGCTAAG	GGATTCTAGAGGTACACAGGAAG
GPX4 promoter-NC (mouse)	ATCCATCTTGTAGTTGCCTGG	AGATCTGACACCCTCTCCTG
GPX4 promoter (mouse)	CAAATGGGAATACAGTGGCTC	CTGAGGCTGGAGTTAGACAC

Supplemental figures and figure legends

Supplemental figure 1

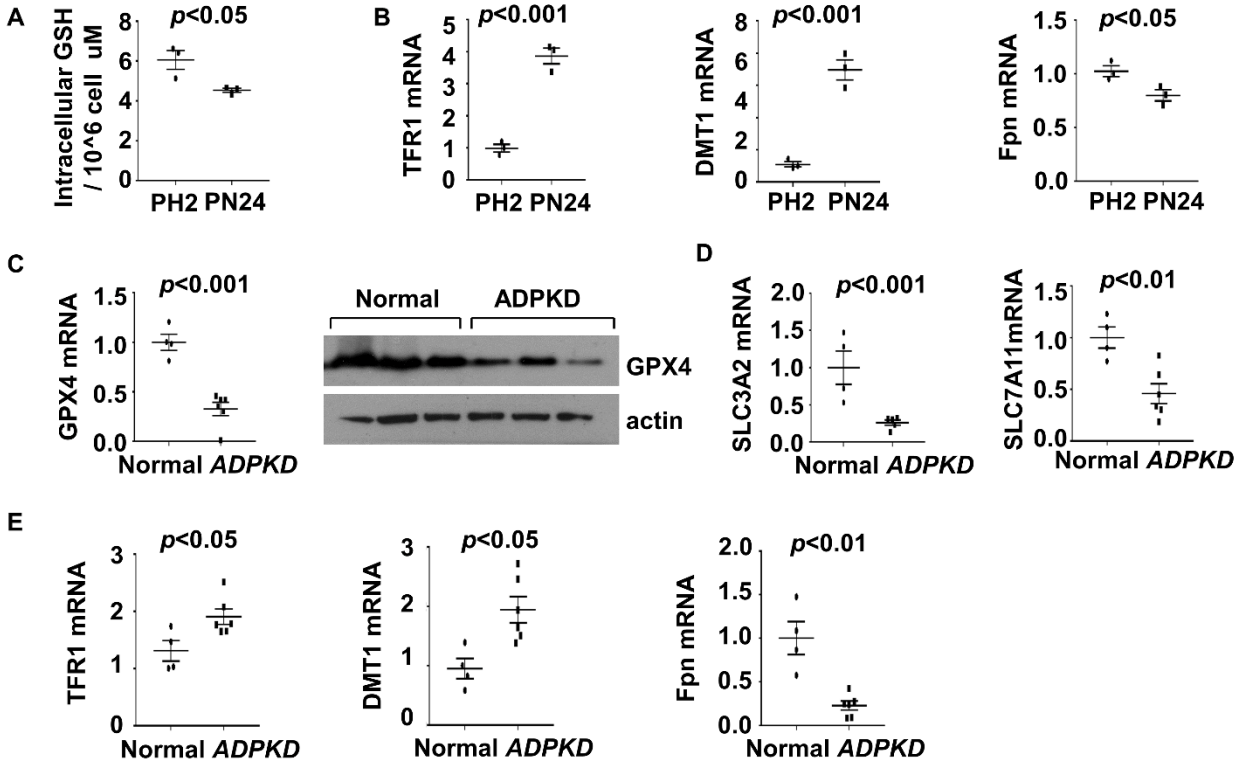

Supplemental figure 1. The expression of ferroptosis related genes was dysregulated in *Pkd1* mutant renal epithelial cells and human ADPKD kidneys. (**A**) Intracellular GSH levels were measured in PH2 and PN24 cells using a colorimetric assay kit (Methods). n = 3 independent experiments. (**B**) qRT-PCR analysis of TFR1, DMT1 and Fpn mRNA levels in PH2 and PN24 cells. n = 3 independent experiments. (**C**) qRT-PCR and Western blot analysis of GPX4 levels in normal human kidneys (n=4) and ADPKD kidneys (n=6). (**D**) qRT-PCR analysis of SLC3A2 and SLC7A11 mRNAs in normal human kidneys (n=4) and ADPKD kidneys (n=6). **(E)** qRT-PCR analysis of TFR1, DMT1 and Fpn mRNAs in normal human kidneys (n=4) and ADPKD kidneys (n=6). Statistical data are presented as the means ± SEM.

Supplemental figure 2

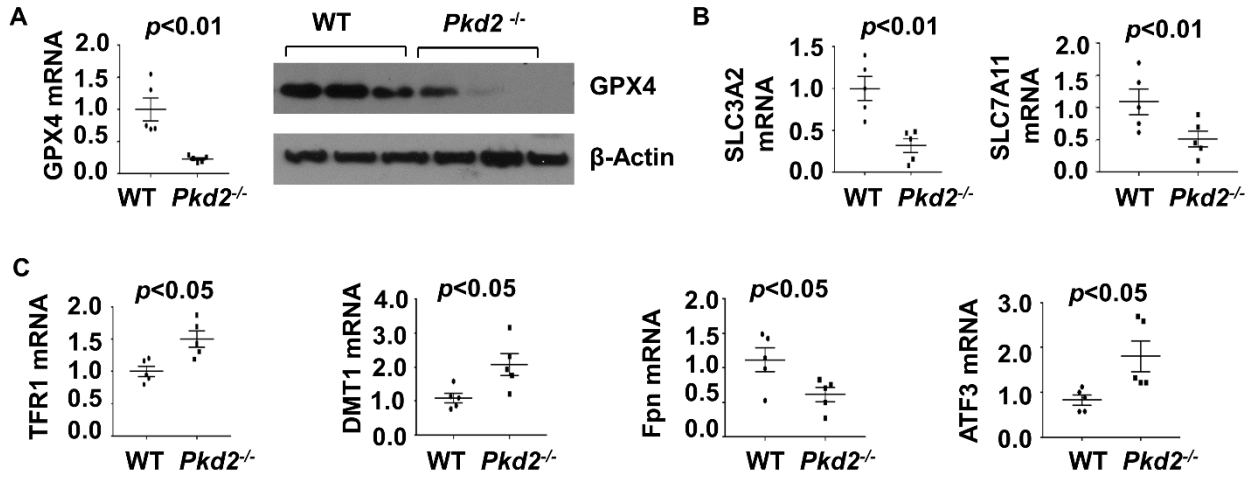

Supplemental figure 2. The expression of ferroptosis related genes was dysregulated in *Pkd2* mutant kidneys. (**A**) qRT-PCR and Western blot analysis of GPX4 levels in wildtype (WT) (n =5) and *Pkd2* mutant kidneys (n=5). (**B**) qRT-PCR analysis of SLC3A2 and SLC7A11 mRNAs in wildtype (WT) (n =5) and *Pkd2* mutant kidneys (n=5). **(C)** qRT-PCR analysis of TFR1, DMT1, Fpn and ATF3 mRNAs in wildtype (WT) (n =5) and *Pkd2* mutant kidneys (n=5). Statistical data are presented as the means ± SEM.

Supplemental figure 3

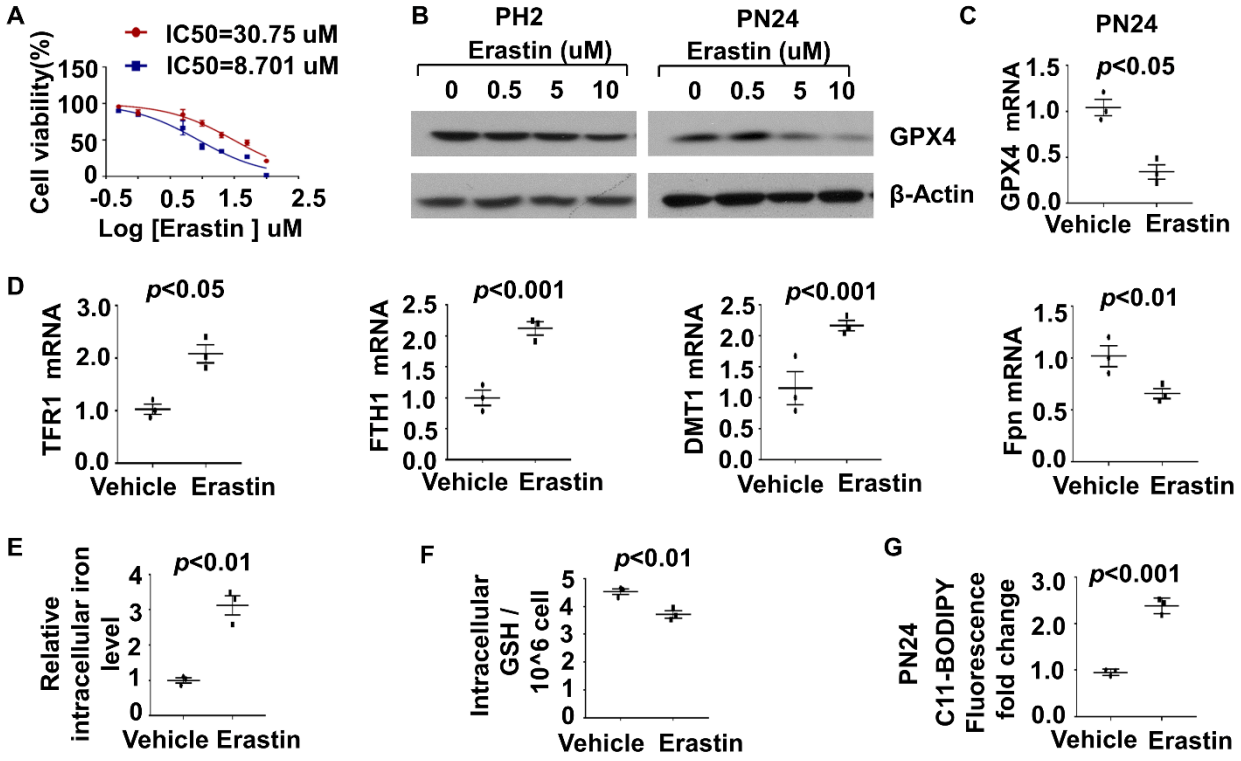

Supplemental figure 3. Depletion of *Pkd1* increases the sensitivity of cystic renal epithelial cells to erastin. (**A**) The IC50 of erastin in PH2 and PN24 cells. n = 3 independent experiments. (**B**) Western blot analysis of GPX4 expression in PH2 and PN24 cells treated with different concentrations of erastin for 24h. (**C**) qRT-PCR analysis of GPX4 mRNA levels in PN24 cells treated with erastin (10 uM) and vehicle for 24h. n = 3 independent experiments. (**D**) qRT-PCR analysis of mRNA levels of TFR1, FTH1, DMT1 and Fpn in PN24 cells treated with erastin (10 uM) and vehicle for 24h. n = 3 independent experiments. (**E**) Intracellular iron levels were measured by an iron assay kit in PN24 cells treated with erastin (10 uM) and vehicle for 24h. n = 3 independent experiments. (**F**) Intracellular GSH levels were measured by a colorimetric assay kit in PN24 cells treated with erastin (10 uM) and vehicle for 24h. n = 3 independent experiments. (**G**) Lipid peroxidation were measured with C11-BODIPY staining PN24 cells treated with erastin (10 uM) and vehicle and quantified with flow cytometry analysis. n = 3 independent experiments. Statistical data are presented as the means ± SEM.

Supplemental figure 4

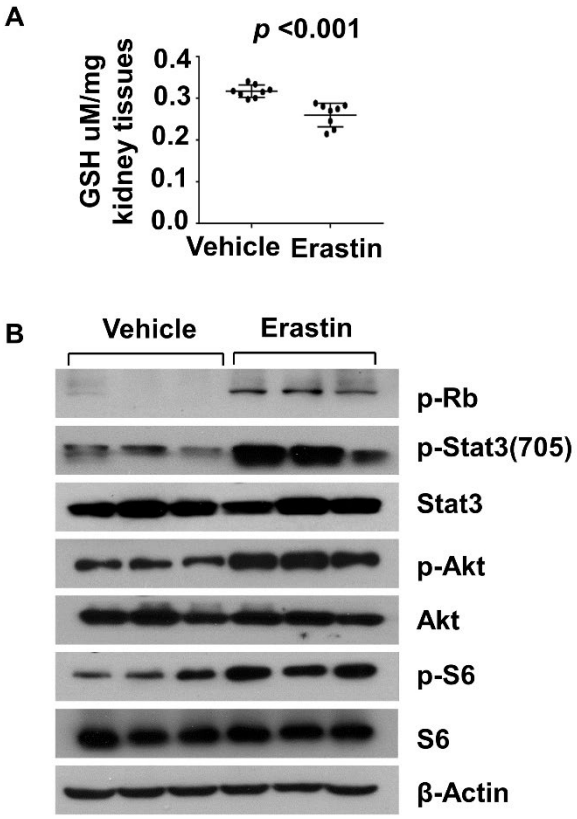

Supplemental figure 4. Treatment with erastin decrease GSH levels but increased cyst-lining epithelial cell proliferation in *Pkd1*$^{RC/RC}$ kidneys. (**A**) The levels of GSH in kidneys from *Pkd1*$^{RC/RC}$ mice treated with erastin (n=8) and vehicle (n=8). (**B**) Western blot analysis of the expression and phosphorylation of Rb, STAT3, Akt, and S6 in kidneys from *Pkd1*$^{RC/RC}$ mice treated with erastin and vehicle. Statistical data are presented as the means ± SEM.

Supplemental figure 5

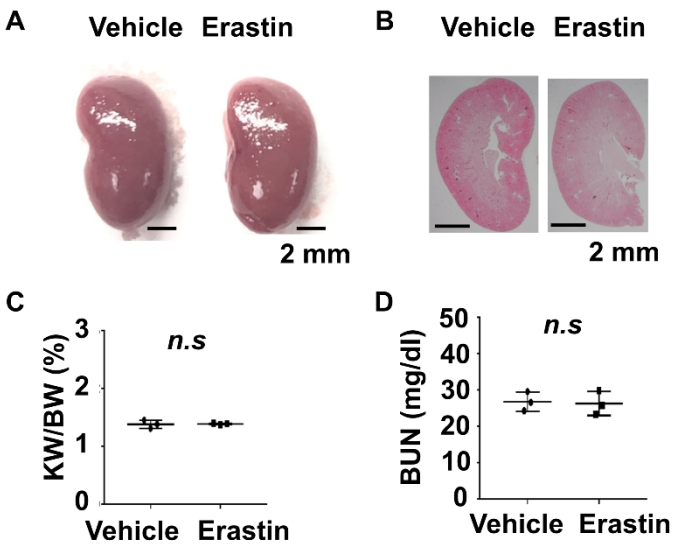

Supplemental figure 5. Treatment with erastin did not promote cyst growth in *Pkd1*$^{RC/+}$ mice kidneys. (A) Representative images of kidneys from *Pkd1*$^{RC/+}$ mice treated with erastin (n=3) or vehicle (n=3) from 1 month to 3 months. Scale bars, 2 mm. (**B**) Histological examination of kidneys from *Pkd1*$^{RC/+}$ mice treated with erastin (n=3) or vehicle (n=3) from 1 month to 3 months. Scale bars: 5 mm. (**C and D)** Treatment with erastin (n=3) did not result in significant changes of KW/BW ratios (**C**) and BUN levels (**D**) in *Pkd1*$^{RC/+}$ mice compared to those in control mice treated with vehicle (n=3). Statistical data are presented as the means ± SEM.

Supplemental figure 6

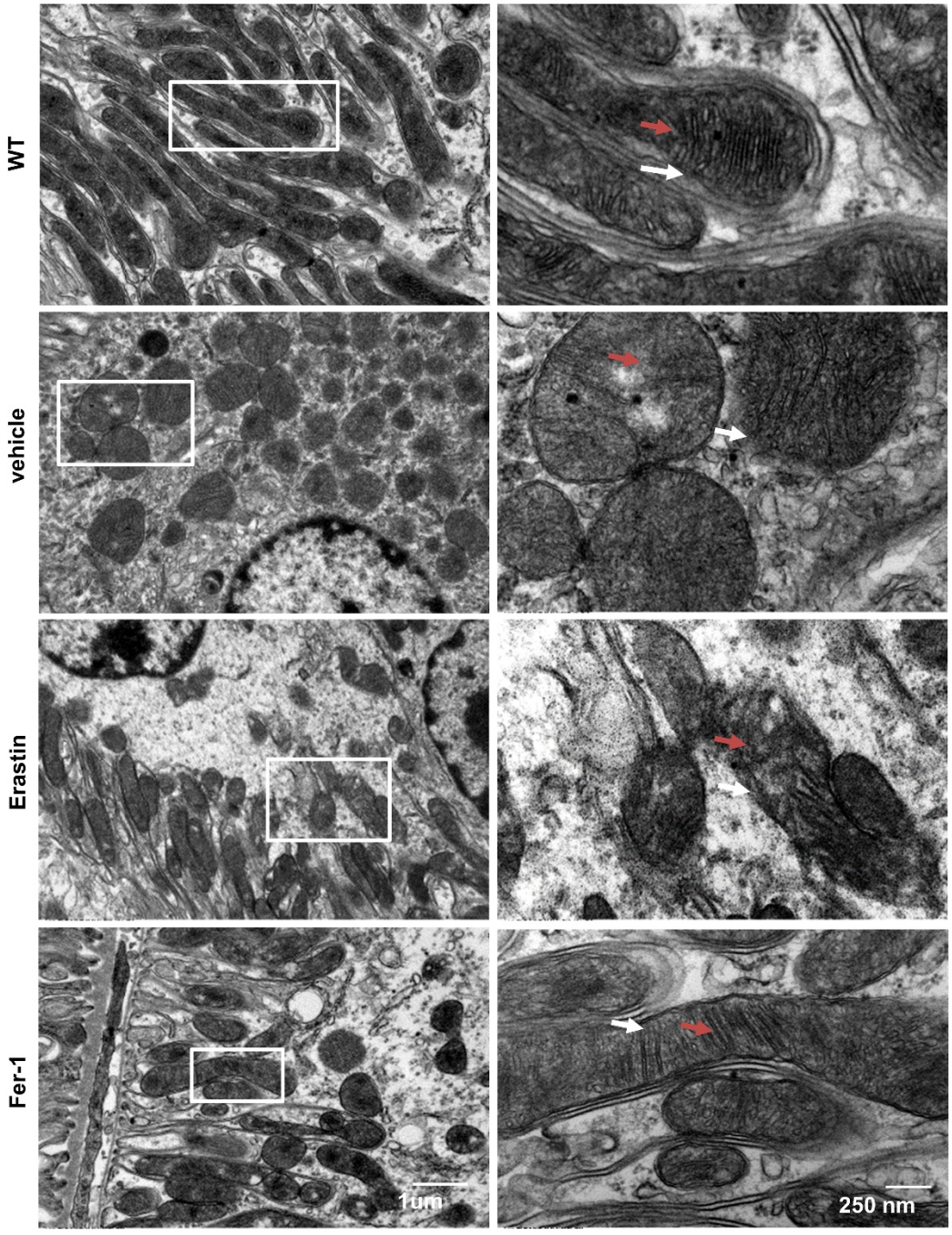

Supplemental figure 6. Mitochondrial morphological and function alteration in *Pkd1* mutant kidneys treated with erastin or Fer-1. Representative transmission electron microscopy images for kidney sections obtained from *Pkd1*$^{RC/RC}$ mice treated with erastin or Fer-1 or vehicle. White arrows indicate the mitochondrial outer membrane and red arrows indicated the mitochondrial crista

Supplemental figure 7

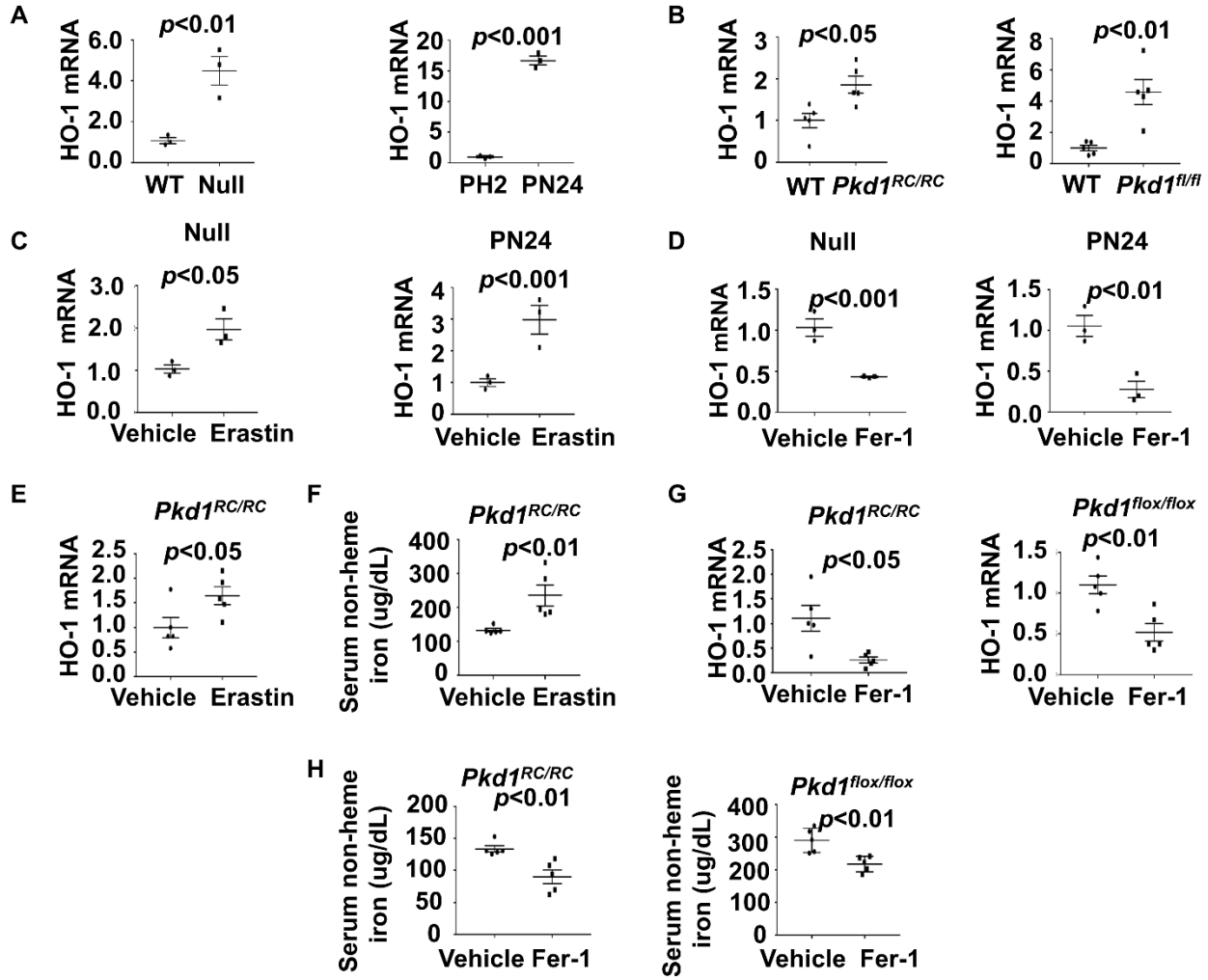

Supplemental figure 7. **Renal and systemic iron metabolism mediated by iron regulatory proteins (IRPs) and heme oxygenase-1 (HO-1) in *Pkd1* mutant kidneys.** (**A**) qRT-PCR analysis of HO-1 mRNA levels in *Pkd1* WT and null MEK cells (*left panel*) as well as in PH2 and PN24 cells (*right panel*). n = 3 independent experiments. (**B**) qRT-PCR analysis of HO-1 mRNA levels in kidneys collected from 3 months old wild type (n=5) and $Pkd1^{RC/RC}$ mice (n=5) (*left panel*) as well as in kidneys collected from 21 days old wild type (n=5) and $Pkd1^{flox/flox}$*:Pkhd1-Cre* mice (n=5) (*right panel*). (**C**) qRT-PCR analysis of HO-1 mRNA levels in *Pkd1* null MEK cells (*left panel*) and PN24 cells (*right panel*) treated with erastin or vehicle. n = 3 independent experiments. (**D**) qRT-PCR analysis of HO-1 mRNA levels in *Pkd1* null MEK cells (*left panel*) and PN24 cells (*right panel*) treated with Fer-1 or vehicle. n = 3 independent experiments. (**E**) qRT-PCR analysis of HO-1 mRNA levels in kidneys collected from 3 months old $Pkd1^{RC/RC}$ mice treated with erastin (n=5) or vehicle (n=5). (**F**) The levels of serum irons in $Pkd1^{RC/RC}$ mice treated with erastin or vehicle. (**G**) qRT-PCR analysis of HO-1 mRNA levels in kidneys collected from 3 months old $Pkd1^{RC/RC}$ mice treated with Fer-1 (n=5) or vehicle (n=5) (*left panel*) and in kidneys collected from 21 days old $Pkd1^{flox/flox}$*:Pkhd1-Cre* mice treated with Fer-1

(n=5) or vehicle (n=5) (*right panel*). (**H**) The levels of serum irons in *Pkd1*$^{RC/RC}$ mice (*left panel*) and *Pkd1*$^{flox/flox}$*:Pkhd1-Cre* mice (*right panel*) treated with Fer-1 or vehicle. Statistical data are presented as the means ± SEM.

Supplemental figure 8

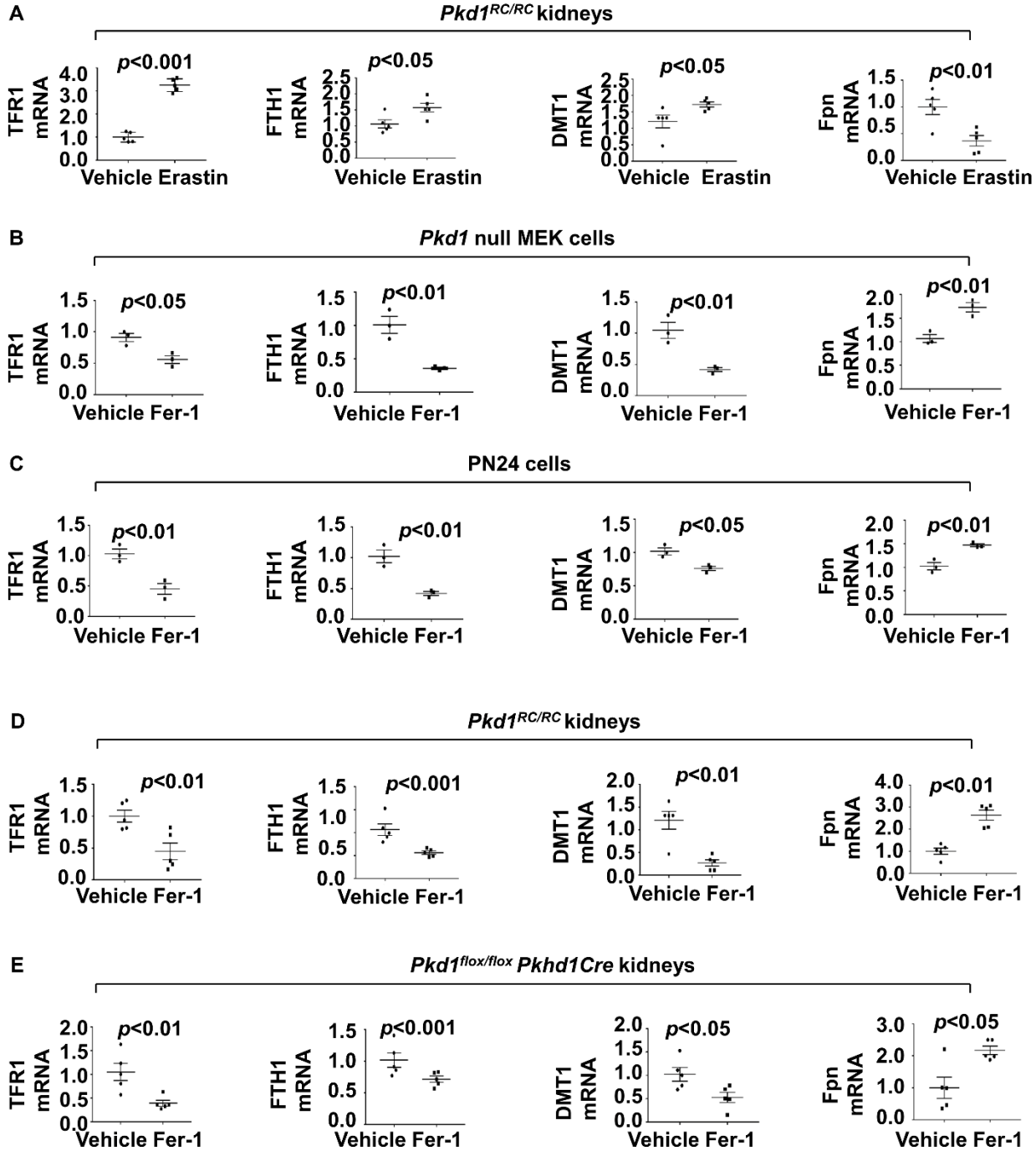

Supplemental figure 8. Iron metabolism associated genes were dysregulated in *Pkd1* mutation renal epithelial cells and tissues treated with erastin or Fer-1. (**A**) qRT-PCR analysis of TFR1, FTH1, DMT1 and Fpn mRNAs in kidneys collected from 3 months old *Pkd1*$^{RC/RC}$ mice treated with erastin (n=5) or vehicle (n=5). (**B**) qRT-PCR analysis of TFR1, FTH1, DMT1 and Fpn mRNAs in *Pkd1* null MEK cells treated with Fer-1 or vehicle. n = 3 independent experiments. (**C**) qRT-PCR analysis of TFR1, FTH1, DMT1 and Fpn mRNAs in PN24 cells treated with Fer-1 or

vehicle. n = 3 independent experiments. (**D**) qRT-PCR analysis of TFR1, FTH1, DMT1 and Fpn mRNAs in kidneys collected from 3 months old *Pkd1*$^{RC/RC}$ mice treated with Fer-1 (n=5) or vehicle (n=5). (**E**) qRT-PCR analysis of TFR1, FTH1, DMT1 and Fpn mRNAs in kidneys collected from 21 days old *Pkd1*$^{flox/flox}$*:Pkhd1-Cre* mice treated with Fer-1 (n=5) or vehicle (n=5). Statistical data are presented as the means ± SEM.

Supplemental figure 9

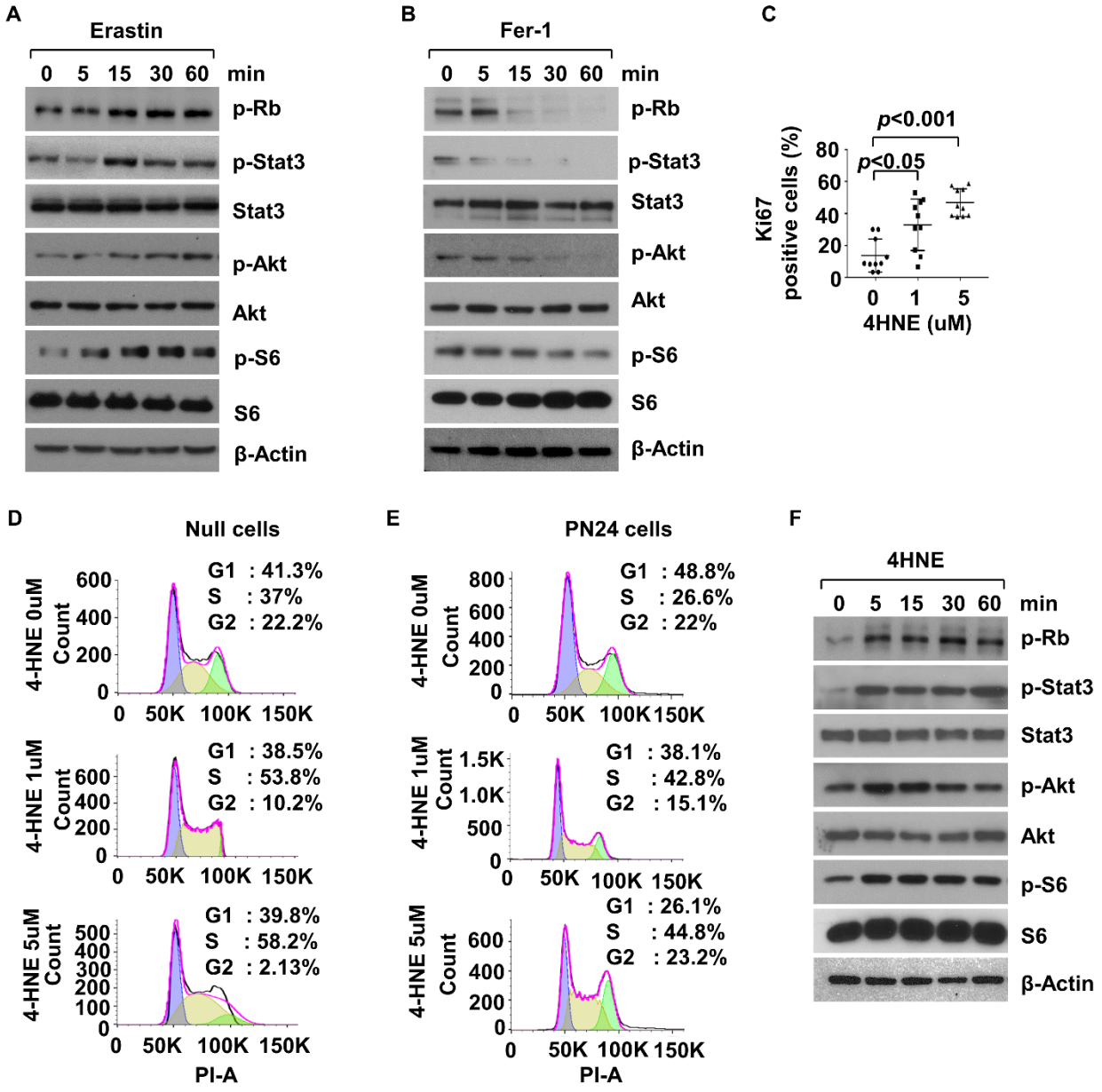

Supplemental figure 9. *Pkd1* mutant renal epithelial cell proliferation was regulated by 4-HNE produced during ferroptotic process. (**A and B**) Western blot analysis of the expression and phosphorylation of Rb, STAT3, Akt, and S6 in PN24 cells treated with erastin (10 μM) (**A**) or Fer-1 (1 uM) (**B**) at indicated time points. (**C**) Ki67 staining indicated that cell proliferation was increased in PN24 cells treated with 4HNE compared to that in those cells treated with vehicle. The percentage of Ki67-positive nuclei of PN24 cells was quantified from an average of 1,000 nuclei per view. (**D and E**) Treatment with 4HNE increases S-phase entry of *Pkd1* null MEK cells (**D**) and PN24 (**E**) cells in a dose dependent manner as examined with flow cytometry analysis. (**E**) Western blot analysis of the expression and phosphorylation of Rb, STAT3, Akt, and S6 in PN24 cells treated with 4HNE (5 uM) at indicated time points. Statistical data are presented as the means ± SEM.

Supplemental figure 10

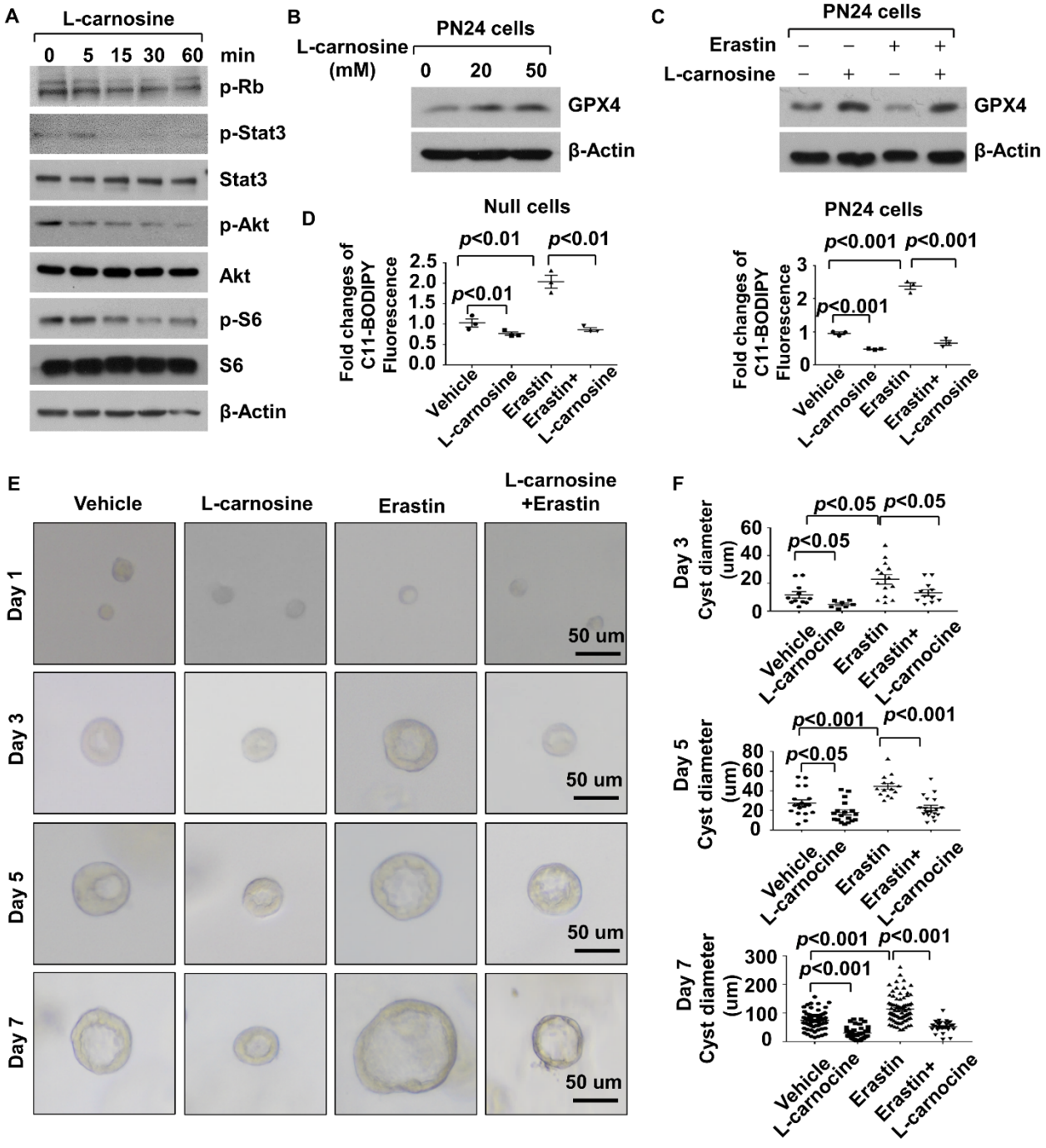

Supplemental figure 10. *Pkd1* mutant renal epithelial cell proliferation was regulated by 4-HNE produced during ferroptotic process. (**A and B**) Western blot analysis of the expression and phosphorylation of Rb, STAT3, Akt, and S6 in *Pkd1* null MEK cells treated with erastin (10 μM) (**A**) or

Fer-1 (1uM) (**B**)at indicated time points. (**C**) Western blot analysis of the expression of 4HNE in *Pkd1* WT and null MEK cells (*left panel*) and PH2, PN24 cells (*right panel*). (**D**) Ki67 staining indicated that cell proliferation was increased in *Pkd1* null MEK cells treated with 4HNE compared to those cells treated with vehicle. The percentage of Ki67-positive nuclei of *Pkd1* null MEK cells was quantified from an average of 1,000 nuclei per field. (**E**) Western blot analysis of the expression and phosphorylation of Rb, STAT3, Akt, and S6 in *Pkd1* null MEK treated with 4HNE (5 uM) at indicated time points. (**F**) Western blot analysis of the expression and phosphorylation of Rb, STAT3, Akt, and S6 in *Pkd1* null MEK cells treated with L-carnosine at indicated time points. (**G and H**) Western blot analysis of the expression of GPX4 in *Pkd1* null MEK cells treated with L-carnosine at indicated concentrations (**G**) and treated with erastin with or without L-carnosine (**H**). Statistical data are presented as the means ± SEM.

Supplemental figure 11

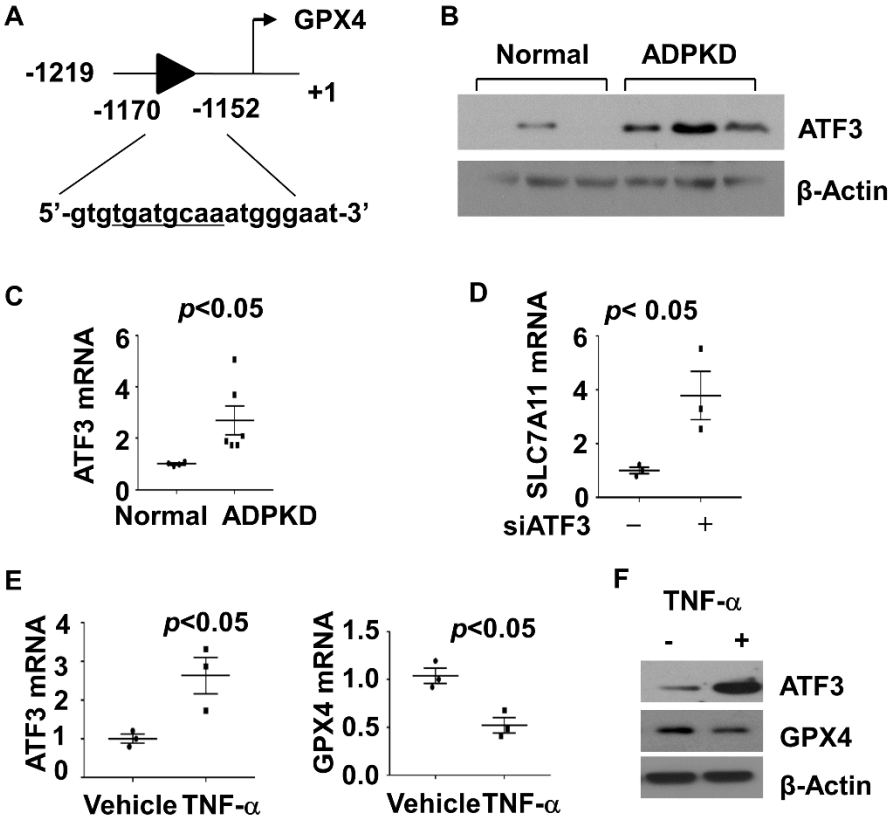

Supplemental figure 11. The expression of GPX4 was regulated by ATF3 in *Pkd1* mutant renal epithelial cells. (A) The localization and the sequence of the ATF3-binding motif in the promoter of GPX4. (**B**) Western blot analysis of ATF3 levels in normal human kidneys and ADPKD kidneys. (**C**) qRT-PCR analysis of ATF3 mRNA level in normal human kidneys (n=4) and ADPKD kidneys (n=6). (**D**) qRT-PCR analysis of SLC7A11 mRNA in PN24 cells transfected with ATF3 siRNA and control siRNA. n = 3 independent experiments. (**E and F**) qRT-PCR and Western blot analysis of ATF3 and GPX4 levels in mIMCD3 cells treated with or without TNF-α. n = 3 independent experiments. Statistical data are presented as the means ± SEM